JOURNAL OF AIRCRAFT
Vol. 34, No. 4, July–August 1997

Panel Flutter Constraints: Analytic Sensitivities and Approximations Including Planform Shape Design Variables

Eli Livne* and David Mineau†
University of Washington, Seattle, Washington 98195-2400

Analytical sensitivities of panel flutter constraints with respect to panel shape as well as thickness and material properties are derived and numerically tested. Cases of fixed in-plane loads and cases in which in-plane loads are variable (depending on panel and overall wing shape as well as material and sizing design variables) are considered. Accuracy of approximations and range of move limits required are studied in preparation for integration with nonlinear programming/approximation concept aeroelastic design synthesis methodology.

Nomenclature

$[A]$ = in-plane local stiffness matrix for the plate, 3×3
$[A_{\text{stiff}}]$, $[A_{\text{damp}}]$ = aerodynamic stiffness and damping matrices, respectively, Eq. (50)
$[\bar{\bar{C}}]$ = damping matrix
D = bending stiffness of isotropic plate
$[D]$ = out-of-plane local stiffness matrix for the plate, 3×3
DV = design variable
$E1$, $E2$, $G12$ = material elastic constants
$F_B(x, y)$ = weight function for admissible functions ensuring zero displacement on panel boundary
$[F_1]$, $[F_2]$, $[F_3]$ = matrices containing admissible functions and their derivatives, Eqs. (9), (19), and (20)
$f_i(x, y)$ = admissible functions
h = total thickness of panel
I_{TR} = integral of a simple polynomial term over trapezoidal panel area
i, i_1, i_2 = indices of terms in layer thickness polynomials
$[K]$, $[K_G]$ = stiffness and geometric stiffness matrix, respectively
$[\bar{\bar{K}}]$ = generalized stiffness matrix including structural and aerodynamic effects, Eqs. (52) and (53)
$[M]$, $[\bar{\bar{M}}]$ = mass matrix
M_∞ = flight Mach number
m, n = powers of x and y in a polynomial term
m_k^{ti}, n_k^{ti} = powers of x and y in polynomial series for thickness of layer i
m_j^v, n_j^v, n_i^u = powers of x and y in polynomial terms of $F_B(x, y)$, Eqs. (3) and (4)
m_p^w, n_p^w = powers of x and y in Ritz functions, Eq. (6)
$[N]$ = 2×2 matrix of in-plane loads
N_i = number of terms in the thickness polynomial for layer i
N_L = number of layers
N_x, N_y, N_{xy} = in-plane loads per unit length
$[\bar{\bar{Q}}]$ = 3×3 constitutive matrix for a layer, Eq. (14)
$[Q_i]$ = material properties matrix, Eq. (13)
$[Q_{\text{stiff}}]$, $[Q_{\text{damp}}]$ = Mach independent aerodynamic stiffness and damping matrices, respectively, Eqs. (43) and (44)
q_D = flight dynamic pressure
$q_{D\text{crit}}$, q_{crit} = critical dynamic pressure
q_P, $\{q\}$ = generalized displacement and the vector of generalized displacements for panel
R, S = coefficients of front line or aft line of panel, Eqs. (1) and (2)
r_{ij} = normalized in-plane loads N_{ij}
s = Laplace variable
T_j^i = coefficient j in the polynomial series for layer i
$t_i(x, y)$ = thickness of layer i
$[\bar{\bar{U}}]$, $[\bar{\bar{V}}]$ = aeroelastic system matrices, Eqs. (55) and (57)
U_i, V_j = shape-dependent coefficients of F_B, Eqs. (3) and (5)
$\tilde{U}_1$–$\tilde{U}_5$ = composite material invariants, Eq. (13)
U_∞ = flight speed
$w^1(x, y)$ = panel elastic out-of-plane displacement
θ = fiber orientation angle
Λ, Ω = normalized dynamic pressure and frequency
λ = eigenvalue
ξ = direction of incoming flow
ρ_m = plate material density
ρ_∞ = air density
ϕ = yaw angle of incoming flow (with respect to x axis)
$\{\phi\}$ = right eigenvector
$\{\psi\}$ = left eigenvector

Subscripts
A = aft (rear)
crit = critical dynamic pressure
F = front
flutter = flutter dynamic pressure
L = left
R = right

Received July 30, 1996; revision received Feb. 28, 1997; accepted for publication March 28, 1997.

*Associate Professor, Department of Aeronautics and Astronautics. Associate Fellow AIAA.
†Graduate Student, Department of Aeronautics and Astronautics.

Introduction

SUBSTANTIAL experience and knowledge have been accumulated over the past four decades regarding the aeroelasticity of panels in supersonic flow.[1–4] Different numerical solution techniques have been used, including exact as well as

approximate Galerkin, Rayleigh-Ritz, and finite element techniques.[5–7] The problem has practical implications associated with the design of high-speed aerospace vehicles. As an aeroelastic research problem, it is rich and interesting, encompassing a wealth of phenomena. These include linear and nonlinear stability and dynamic response, dynamics of systems with random parameters,[8] and interactions between static and dynamic instabilities in the presence of in-plane loads and thermal effects.[9,10] Panel flutter has been used to study applications of composite materials,[11,12] transverse shear effects,[13,14] active aeroelastic control using strain actuators,[15,16] chaotic dynamics,[17,18] and order reduction in unsteady aerodynamics.[19] Most of the studies in the vast panel flutter literature, however, are confined to rectangular panels. Solution techniques and results for quadrilateral and trapezoidal panels have been discussed in only a small number of articles.[20–23]

Skin panels in typical aerospace structures, however, are very often trapezoidal in shape. Moreover, in the course of shape optimization of such aerospace structures, internal ribs, spars, and stiffeners may be moved to form trapezoidal skin panels (Fig. 1), and these panels may change shape during optimization in addition to changing material properties and thicknesses. The capability to efficiently evaluate the aeroelastic stability of trapezoidal skin panels under combined in-plane loads, as well as sensitivities with respect to sizing, material, and shape design variables, constitutes an important building block in any overall structural/aeroelastic optimization capability. For optimization strategies based on nonlinear programming and approximation concepts,[24] evaluation of alternative approximation techniques for aeroelastic constraints is required, since very little experience exists in this area.

The optimization of panels, subject to aeroelastic constraints, has been studied in cases involving isotropic and composite construction.[25–29] These studies are usually limited to the treatment of an isolated rectangular panel, excluding its interaction with the structure containing it. In the effort to develop effective aeroservoelastic synthesis techniques for stressed skin aerospace structures, the area of airframe shape optimization becomes important, because of the need to make rigorous design optimization available to the designer at an early stage of the design process, where overall shape of the vehicle is still evolving. Analytic shape sensitivities and approximations have been developed for wing box structural modeling,[30,31] integrated wing box/panel buckling analysis,[32] panel vibrations,[33] and unsteady wing aerodynamics in both subsonic and supersonic flight.[34,35] This paper focuses on the integrated wing box/panel flutter analysis and sensitivity problem with an emphasis on the needs of planform shape optimization. This includes, as a special case, the shape sensitivity analysis of panel flutter in the case of the isolated panel, subject to given fixed in-plane loads.

In optimized modern aerospace structures, buckling constraints are active in many skin panels. The ratio of actual in-plane loads to buckling in-plane loads can have a significant effect on the aeroelastic stability of a panel. Thus, the construction of panel stability constraints that account for the interaction between buckling and flutter is an important addition to the set of constraints used in multidisciplinary aerospace vehicle synthesis.

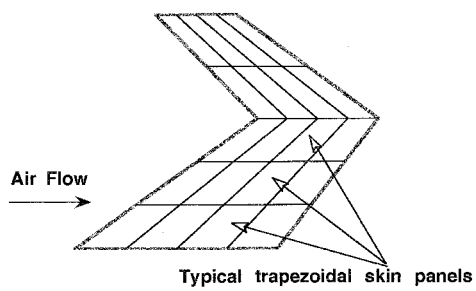

Fig. 1 Wing planform and typical skin panels.

This paper begins with a discussion of panel modeling and the use of simple polynomials as admissible functions in the Ritz analysis. It is shown how this formulation leads to the expression of mass, stiffness, geometric stiffness, and aerodynamic matrix terms as linear combinations of members of a single table of area integrals, obtained explicitly over the planform area of the panel. Analytic sensitivities with respect to panel shape, thickness, and fiber orientation are derived. Test cases and results conclude the presentation. Detailed derivations, a more complete set of results, and discussion of the computer program developed for this work can be found in Ref. 36.

Simple Polynomials for Modeling and Shape Sensitivities

It has been shown how skin panel buckling analysis can be integrated with wing box structural analysis for design oriented structural analysis (DOSA) of wing structures, including analytic sensitivities and approximations.[32] Emphasis was placed on planform shape optimization. In this work, the techniques of Ref. 32 are extended to include panel flutter in supersonic flow. The linearized panel flutter problem is treated here. Simply supported boundary conditions are assumed, although edge rotational stiffness can be introduced without much difficulty.

Figure 2 shows a trapezoidal panel defined by coordinates of its vertices in the x, y axes. The x coordinates of the forward and rear points on a line parallel to the sides of the panel are x_F and x_A, respectively. Based on Fig. 2, we can write the following equation for points on the front line:

$$x_F(y) = \left(\frac{x_{FL}y_R - x_{FR}y_L}{y_R - y_L}\right) + \left(\frac{x_{FR} - x_{FL}}{y_R - y_L}\right) y$$
$$x_F(y) = R_F + S_F y \tag{1}$$

In a similar way, on the rear line, expressing x_A in terms of y leads to

$$x_A(y) = \left(\frac{x_{AL}y_R - x_{AR}y_L}{y_R - y_L}\right) + \left(\frac{x_{AR} - x_{AL}}{y_R - y_L}\right) y$$
$$x_A(y) = R_A + S_A y \tag{2}$$

The following function satisfies the zero displacement boundary conditions on the circumference of the panel:

$$F_B(x, y) = [x - x_F(y)][x - x_A(y)][y - y_L][y - y_R]$$

Using Eqs. (1) and (2) and expanding in terms of x and y yields

$$F_B(x, y) = (U_1 + U_2 y + U_3 y^2) \times \{V_1 + V_2 x + V_3 y + V_4 x^2 + V_5 xy + V_6 y^2\} \tag{3}$$

and, using the index notation

$$F_B(x, y) = \sum_{i=1}^{3} U_i y^{n_i^u} \sum_{j=1}^{6} V_j x^{m_j^v} y^{n_j^v} = \sum_{i=1}^{3} \sum_{j=1}^{6} U_i V_j x^{m_j^v} y^{n_i^u + n_j^v} \tag{4}$$

where the constants U and V are given explicitly in terms of panel vertex coordinates by

$$U_1 = y_L y_R, \quad U_2 = -(y_L + y_R), \quad U_3 = 1$$
$$V_1 = R_A R_F, \quad V_2 = -(R_A + R_F), \quad V_3 = (R_A S_F + R_F S_A) \tag{5}$$
$$V_4 = 1, \quad V_5 = -(S_A + S_F), \quad V_6 = S_F S_A$$

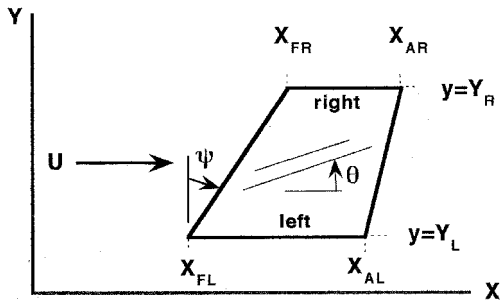

Fig. 2 Planform geometry of a trapezoidal panel.

Multiplying the weight function $F_B(x, y)$ by a general simple polynomial series, admissible displacement functions for the simply supported trapezoidal panel are obtained

$$w^1(x, y) = F_B(x, y) \sum_{p=1}^{N_W} q_p x^{m_p^w} y^{n_p^w} \tag{6}$$

where the coefficients $q_p(t)$ are the generalized displacements, and $w^1(x, y)$ is the vertical displacement of the panel. Substituting the expression for $F_B(x, y)$ from Eq. (4), we can write

$$w^1(x, y) = \sum_{p=1}^{N_W} q_p \cdot \sum_{i=1}^{3} \sum_{j=1}^{6} U_i V_j x^{(m_j^v + m_p^w)} y^{(n_i^u + n_j^v + n_p^w)} \tag{7}$$

The admissible functions are thus expressed in terms of simple polynomials, where the pth admissible function is given by

$$f_p(x, y) = \sum_{i=1}^{3} \sum_{j=1}^{6} U_i V_j x^{(m_j^v + m_p^w)} y^{(n_i^u + n_j^v + n_p^w)} \tag{8}$$

The unknown elastic panel deflection $w^1(x, y)$ is approximated by a series of admissible functions:

$$w^1(x, y) = \sum_{p=1}^{N} f_p(x, y) q_p = \{f_1(x, y) \quad f_2(x, y) \quad \cdots \quad f_N(x, y)\} \times \begin{Bmatrix} q_1 \\ q_2 \\ \vdots \\ q_N \end{Bmatrix} = [F_1(x, y)]\{q\} \tag{9}$$

In a polynomial-based equivalent plate[30,37] wing box analysis, the thickness of layers of fibers in different directions is given by simple polynomials. For layer i (out of N_L layers)

$$t_i(x, y) = T_1^i + T_2^i x + T_3^i y + T_4^i x^2 + \cdots = \sum_{k=1}^{N_i} T_k^i \cdot x^{(m_k^t)} \cdot y^{(n_k^t)} \qquad i = 1, N_L \tag{10}$$

The powers m_k^t and n_k^t are x and y powers of the kth term of the thickness series for the ith layer. The coefficients T_k^i serve as sizing-type design variables. The same parametrization of thickness distribution can be used in finite element-based wing design synthesis,[31] and in this case the coefficients T_k^i serve as linking design variables.[24]

Unlike many studies, in which wing trapezoidal segments are transformed into a unit square for numerical integrations, here the thickness polynomial is given in terms of the physical x, y coordinates (Fig. 2). The overall thickness of skin panels is given by (Eq. 10):

$$h(x, y) = \sum_{i=1}^{N_L} t_i(x, y) = \sum_{i=1}^{N_L} \sum_{k=1}^{N_i} T_k^i \cdot x^{(m_k^t)} \cdot y^{(n_k^t)} \tag{11}$$

In a similar manner, cap areas for the spars and ribs of the wing box model are also expressed as simple polynomials of either x (for ribs) or y (for spars). Depth of the wing box is also given by a simple polynomial in x and y (Refs. 30 and 37).

The ability to describe thickness distribution, wing box deformations, and panel deformations in terms of simple polynomials in x and y makes it possible to obtain stiffness, geometric stiffness, mass, and unsteady aerodynamic generalized force matrices analytically without any numerical quadrature. For example, in the case of stiffness terms, polynomial description of skin-layer thicknesses in terms of the global x-y coordinates was given in Eqs. (10) and (11). For a panel containing N_L layers of fibers, $[A]$ can be expressed in terms of individual layer thicknesses and fiber orientation angles as

$$[A] = \sum_{i=1}^{N_L} [\bar{\bar{Q}}(\theta_i)] \cdot t_i(x, y) = \sum_{i=1}^{N_L} \langle [Q_0] + [Q_1]\cos 2\theta_i + [Q_2]\cos 4\theta_i + [Q_3]\sin 2\theta_i + [Q_4]\sin 4\theta_i \rangle \cdot t_i(x, y) \tag{12}$$

where the matrices $[Q_0]$ to $[Q_4]$ depend on material invariants, $\tilde{U}_1 - \tilde{U}_5$. Let

$$[Q] = \begin{bmatrix} \tilde{U}_1 & \tilde{U}_4 & 0 \\ \tilde{U}_4 & \tilde{U}_1 & 0 \\ 0 & 0 & \tilde{U}_5 \end{bmatrix} + \tilde{U}_2 \begin{bmatrix} 1 & 0 & 0 \\ 0 & -1 & 0 \\ 0 & 0 & 0 \end{bmatrix} \cos(2\theta) + \tilde{U}_3 \begin{bmatrix} 1 & -1 & 0 \\ -1 & 1 & 0 \\ 0 & 0 & -1 \end{bmatrix} \cos(4\theta) + \frac{\tilde{U}_2}{2} \begin{bmatrix} 0 & 0 & 1 \\ 0 & 0 & 1 \\ 1 & 1 & 0 \end{bmatrix} \times \sin(2\theta) + \tilde{U}_3 \begin{bmatrix} 0 & 0 & 1 \\ 0 & 0 & -1 \\ 1 & -1 & 0 \end{bmatrix} \sin(4\theta) \tag{13}$$

Now, let a material and fiber orientation dependent $[\bar{\bar{Q}}(\theta_i)]$, a 3×3 matrix, be defined as

$$[\bar{\bar{Q}}(\theta_i)] = [Q_0] + [Q_1]\cos 2\theta_i + [Q_2]\cos 4\theta_i + [Q_3]\sin 2\theta_i + [Q_4]\sin 4\theta_i \tag{14}$$

$[A]$ can now be expressed in terms of the sizing design variables T_j^i and fiber directions as a polynomial:

$$[A] = \sum_{i=1}^{N_L} \sum_{k=1}^{N_i} [\bar{\bar{Q}}(\theta_i)] \cdot x^{(m_k^t)} \cdot y^{(n_k^t)} \cdot T_k^i \tag{15}$$

For unidirectional, orthotropic, or quasihomogeneous laminates,[32] the in-plane and bending stiffness matrices are related through

$$[D] = [A](h^2/12) \tag{16}$$

Using Eq. (11) to express the square of the total panel thickness h^2, in terms of sizing-type design variables, double summation is needed. The indices l_1 and l_2 are used for summation of polynomial terms associated with each layer, as follows:

$$h(x, y) = \sum_{i1=1}^{N_L} \sum_{l1=1}^{N_{i1}} T_{l1}^{i1} \cdot x^{(m_{l1}^t)} \cdot y^{(n_{l1}^t)}$$
$$h(x, y) = \sum_{i2=1}^{N_L} \sum_{l2=1}^{N_{i2}} T_{l2}^{i2} \cdot x^{(m_{l2}^t)} \cdot y^{(n_{l2}^t)} \tag{17}$$

The bending stiffness matrix $[D]$ can now be written in polynomial form as

$$[D] = [A]\frac{h^2}{12} = \frac{1}{12} \sum_{i=1}^{N_L} [\bar{\bar{Q}}(\theta_i)] \sum_{i1=1}^{N_L} \sum_{i2=1}^{N_L} \sum_{k=1}^{N_i} \sum_{l1=1}^{N_{i1}} \sum_{l2=1}^{N_{i2}} \times \langle T_k^i \cdot T_{l1}^{i1} \cdot T_{l2}^{i2} \cdot x^{(m_k^t + m_{l1}^t + m_{l2}^t)} y^{(n_k^t + n_{l1}^t + n_{l2}^t)} \rangle \tag{18}$$

For stiffness and geometric stiffness matrix evaluation, first and second derivatives with respect to x and y of the vertical deformation are needed. The first derivatives, then, can be expressed as

$$\begin{Bmatrix} w^1_{,x} \\ w^1_{,y} \end{Bmatrix} = \begin{bmatrix} f_{1,x} & f_{2,x} & \cdots & f_{N,x} \\ f_{1,y} & f_{2,y} & \cdots & f_{N,y} \end{bmatrix} \begin{Bmatrix} q_1 \\ q_2 \\ \cdot \\ q_N \end{Bmatrix} = [F_2]\{q\} \tag{19}$$

and the second derivatives are given by

$$\begin{Bmatrix} w^1_{,xx} \\ w^1_{,yy} \\ 2w^1_{,xy} \end{Bmatrix} = \begin{bmatrix} f_{1,xx} & f_{2,xx} & \cdots & f_{N,xx} \\ f_{1,yy} & f_{2,yy} & \cdots & f_{N,yy} \\ 2f_{1,xy} & 2f_{2,xy} & \cdots & 2f_{N,xy} \end{bmatrix} \begin{Bmatrix} q_1 \\ q_2 \\ \cdot \\ q_N \end{Bmatrix} = [F_3]\{\boldsymbol{q}\} \tag{20}$$

In Eqs. (9), (19), and (20), the matrices $[F_1]$, $[F_2]$, and $[F_3]$ are all functions of x and y. It is shown in Refs. 32 and 36 that the generalized stiffness and geometric stiffness matrices for the trapezoidal panel, corresponding to the polynomial Ritz functions in Eqs. (8) and (9) are obtained by surface integration over the area of the panel. The stiffness matrix is given by

$$[K]_{N\times N} = \int\int [F_3]^T[D][F_3]\,\mathrm{d}x\,\mathrm{d}y \tag{21}$$

and the geometric stiffness matrix is given by

$$[K_G]_{N\times N} = \int\int [F_2]^T[N][F_2]\,\mathrm{d}x\,\mathrm{d}y \tag{22}$$

where the matrix $[N]$ contains the in-plane loads acting on the panel

$$[N] = \begin{bmatrix} N_{xx} & N_{xy} \\ N_{xy} & N_{yy} \end{bmatrix} \tag{23}$$

These in-plane loads are functions of x and y and are available in simple polynomial form, whether as a result of wing box analysis based on a polynomial equivalent plate approach[32] or by least-square fitting of simple polynomial functions to the in-plane load distribution calculated by any finite element analysis of the wing box.[31]

Elements of the matrices $[F_1]$, $[F_2]$, and $[F_3]$, as well as $[D]$ and $[N]$, are all simple polynomial functions of x and y (Ref. 32). The area integrations in Eqs. (21) and (22) lead to integrals of simple polynomial functions over trapezoidal areas. As shown in Ref. 30, these integrals can be evaluated analytically in closed form, and thus, no numerical quadrature is required. Once a table of area integrals of the following form is prepared for a panel, all elements of the stiffness matrix and the geometric stiffness matrix are linear combinations of members of this table of integrals, as shown in Ref. 32:

$$I_{\mathrm{TR}}(m, n) = \int\int_{\mathrm{area}} x^m y^n\,\mathrm{d}x\,\mathrm{d}y \tag{24}$$

Mass Matrix

When the kinetic energy of the panel in transverse motion is expressed in terms of the Ritz functions [Eq. (9)], the mass matrix is found to be

$$[M] = \int\int_{\mathrm{area}} \rho_m h[F_1]^T[F_1]\,\mathrm{d}x\,\mathrm{d}y \tag{25}$$

where ρ_m is the material density, $h(x, y)$ is the panel thickness, and the matrix $[F_1]$ [Eq. (9)] contains the admissible functions, and is, thus, also a function of (x, y). The rs element of the mass matrix is given by

$$M_{\mathrm{rs}} = \int\int_{\mathrm{area}} \rho_m h f_r f_s\,\mathrm{d}x\,\mathrm{d}y \tag{26}$$

The thickness series used for the different skin layers [Eqs. (10) and (11)] shows that if the thickness distributions of all layers are expressed by complete polynomials of the same order, then all layers will have the same number of terms N_t and the same powers m^t_k and n^t_k in their respective thickness series. This simplifies the formulation of the panel thickness while not taking away from the flexibility to represent complex panel thickness distributions. A new vector of thickness coefficients $\overline{\boldsymbol{T}}_k$ is defined to add all of the T^i_k terms associated with the same powers of x and y:

$$\overline{\boldsymbol{T}}_k = \sum_{i=1}^{N_L} T^i_k \tag{27}$$

Now the total panel thickness is expressed as

$$h(x, y) = \sum_{k=1}^{N_t} \overline{\boldsymbol{T}}_k x^{m^t_k} y^{n^t_k} \tag{28}$$

Substituting this into Eq. (26) leads to

$$M_{\mathrm{rs}} = \rho_m \sum_{k=1}^{N_t} \overline{T}_k \int\int_{\mathrm{area}} f_r f_s x^{m^t_k} y^{n^t_k}\,\mathrm{d}x\,\mathrm{d}y \tag{29}$$

When the polynomial admissible Ritz functions [Eq. (8)] are used in Eq. (29), then the explicit form of mass matrix elements is obtained

$$M_{\mathrm{rs}} = \rho_m \cdot \sum_{k=1}^{N_t} \sum_{i=1}^{3} \sum_{j=1}^{6} \sum_{ii=1}^{3} \sum_{jj=1}^{6} \overline{\boldsymbol{T}}_k U_i V_j U_{ii} V_{jj} \int\int_{\mathrm{area}} x^m y^n\,\mathrm{d}x\,\mathrm{d}y \tag{30}$$

where the powers m and n are

$$\begin{aligned} m &= m^v_j + m^v_{jj} + m^w_r + m^w_s + m^t_k \\ n &= n^u_i + n^u_{ii} + n^v_j + n^v_{jj} + n^w_r + n^w_s + n^t_k \end{aligned} \tag{31}$$

Note that all of the elements of the mass matrix are linear combinations of area integrals $I_{\mathrm{TR}}(m, n)$ of simple polynomials [Eq. (24)] over the trapezoidal panel. The mass matrix is dependent on the material density, the thickness terms T^i_k (through $\overline{\boldsymbol{T}}_k$), and the panel shape variables (through U_i and V_j). The area integrals depend only on the panel shape variables through the limits of integration.[32]

Aerodynamic Force Matrices

When virtual work due to surface pressure difference distribution $\Delta p(x, y)$ is expressed in terms of the Ritz functions [Eqs. (8) and (9)], the vector of generalized aerodynamic forces is obtained:

$$\{\boldsymbol{Q}_A\} = \int\int_{\mathrm{area}} [F_1]^T \Delta p(x, y)\,\mathrm{d}x\,\mathrm{d}y \tag{32}$$

First-order linear piston theory[1,2] approximates $\Delta p(x, y)$ by

$$\Delta p = \frac{\rho_\infty U^2_\infty}{\sqrt{M^2_\infty - 1}} \left\{ w^1_{,\xi} + \frac{M^2_\infty - 2}{M^2_\infty - 1} \frac{1}{U_\infty} w^1_{,t} \right\} \tag{33}$$

where ρ_∞, U_∞, and M_∞ are the freestream density, velocity, and Mach number, respectively, and ξ is the flow direction.

Panels are aligned so that their left and right sides are parallel to the x axis (Fig. 2). When the in-coming flow is yawed with respect to the x axis (creating an angle ϕ with the x axis), then the slope of panel deformation along the flow direction ξ is given by

$$\frac{\partial}{\partial \xi} = \cos\phi \frac{\partial}{\partial x} + \sin\phi \frac{\partial}{\partial y} \tag{34}$$

The pressure difference according to first-order piston theory can now be rewritten as

$$\Delta p(x, y, t) = P_\xi \cos\phi w^1_{,x} + P_\xi \sin\phi w^1_{,y} + P_t w^1_{,t} \tag{35}$$

where

$$P_\xi = \frac{\rho_\infty U_\infty^2}{\sqrt{M_\infty^2 - 1}} \tag{36}$$

$$P_t = P_\xi \frac{M_\infty^2 - 2}{M_\infty^2 - 1} \frac{1}{U_\infty} \tag{37}$$

Equation (9) is now differentiated with respect to x and then with respect to y

$$w^1_{,x}(x, y) = \{f_{1,x} \quad f_{2,x} \quad \cdots \quad f_{N,x}\} \begin{Bmatrix} q_1 \\ q_2 \\ \cdot \\ q_N \end{Bmatrix} = [F_{1,x}]\{\boldsymbol{q}\} \tag{38}$$

$$w^1_{,y}(x, y) = \{f_{1,y} \quad f_{2,y} \quad \cdots \quad f_{N,y}\} \begin{Bmatrix} q_1 \\ q_2 \\ \cdot \\ q_N \end{Bmatrix} = [F_{1,y}]\{\boldsymbol{q}\} \tag{39}$$

Differentiation with respect to time leads to

$$w_{,t}(x, y) = \{f_1 \quad f_2 \quad \cdots \quad f_N\} \begin{Bmatrix} q_{1,t} \\ q_{2,t} \\ \cdot \\ q_{N,t} \end{Bmatrix} = [F_1]\{\boldsymbol{q}_{,t}\} \tag{40}$$

and substituting Eqs. (38–40) into Eq. (35) gives

$$\{\boldsymbol{Q}_A\} = P_\xi \cos\phi \int\int_{\text{area}} [F_1]^T[F_{1,x}]\{\boldsymbol{q}\}\, dx\, dy + P_\xi \sin\phi \int\int_{\text{area}} [F_1]^T[F_{1,y}]\{\boldsymbol{q}\}\, dx\, dy + P_t \int\int_{\text{area}} [F_1]^T[F_1]\{\boldsymbol{q}_{,t}\}\, dx\, dy \tag{41}$$

It is natural at this point to define an aerodynamic stiffness matrix and an aerodynamic damping matrix:

$$\{\boldsymbol{Q}_A\} = P_\xi[Q_{\text{stiff}}]\{\boldsymbol{q}\} + P_t[Q_{\text{damp}}]\{\boldsymbol{q}_{,t}\} \tag{42}$$

where the rs elements are given by

$$Q_{\text{stiff}\,rs} = \cos\phi \int\int_{\text{area}} f_r f_{s,x}\, dx\, dy + \sin\phi \int\int_{\text{area}} f_r f_{s,y}\, dx\, dy \tag{43}$$

$$Q_{\text{damp}\,rs} = \int\int_{\text{area}} f_r f_s\, dx\, dy \tag{44}$$

f_r and f_s are the rth and sth admissible functions [Eq. (8)]. The first derivatives of the admissible functions (with respect to x and y) are

$$f_{p,x} = \sum_{i=1}^{3}\sum_{j=1}^{6} U_i V_j (m_j^v + m_p^w) x^{(m_j^v + m_p^w - 1)} y^{(n_i^u + n_j^v + n_p^w)} \tag{45}$$

$$f_{p,y} = \sum_{i=1}^{3}\sum_{j=1}^{6} U_i V_j (n_i^u + n_j^v + n_p^w) \cdot x^{(m_j^v + m_p^w)} y^{(n_i^u + n_j^v + n_p^w - 1)} \tag{46}$$

Substituting these into Eqs. (43) and (44) leads to the final expression for the elements of the aerodynamic damping and stiffness matrices:

$$Q_{\text{stiff}\,rs} = \cos\phi \sum_{i=1}^{3}\sum_{j=1}^{6}\sum_{ii=1}^{3}\sum_{jj=1}^{6} U_i V_j U_{ii} V_{jj} \cdot (m_{jj}^v + m_s^w) \times \int\int_{\text{area}} x^{m-1} y^n\, dx\, dy + \sin\phi \sum_{i=1}^{3}\sum_{j=1}^{6}\sum_{ii=1}^{3}\sum_{jj=1}^{6} U_i V_j U_{ii} V_{jj} \times (n_{ii}^u + n_{jj}^v + n_s^w) \int\int_{\text{area}} x^m y^{n-1}\, dx\, dy \tag{47}$$

$$Q_{\text{damp}\,rs} = \sum_{i=1}^{3}\sum_{j=1}^{6}\sum_{ii=1}^{3}\sum_{jj=1}^{6} U_i V_j U_{ii} V_{jj} \int\int_{\text{area}} x^m y^n\, dx\, dy \tag{48}$$

where the powers m, n are given by

$$\begin{aligned} m &= (m_j^v + m_{jj}^v + m_r^w + m_s^w) \\ n &= (n_i^u + n_{ii}^u + n_j^v + n_{jj}^v + n_r^w + n_s^w) \end{aligned} \tag{49}$$

The elements of the aerodynamic stiffness and damping matrices are, thus, linear combinations of the same area integrals [Eq. (24)] as the mass, stiffness, and geometric stiffness matrices. The aerodynamic stiffness matrix is dependent on the airstream yaw angle ϕ, the dynamic pressure and Mach number through P_ξ, and the panel shape variables through U_i and V_j. The aerodynamic damping matrix is dependent on the dynamic pressure and Mach number through P_t, and on the panel shape variables through U_i and V_j. Of course, the area integrals, $I_{TR}(m, n)$ themselves also depend on the panel's planform shape variables.

For aeroelastic stability analysis, as shown in the following, it is convenient to express the aerodynamic matrices in the form

$$\begin{aligned} [A_{\text{stiff}}] &= \frac{1}{\sqrt{M_\infty^2 - 1}} [Q_{\text{stiff}}] \\ [A_{\text{damp}}] &= \frac{1}{\sqrt{M_\infty^2 - 1}} \frac{M_\infty^2 - 2}{M_\infty^2 - 1} [Q_{\text{damp}}] \end{aligned} \tag{50}$$

which leads to an expression for the aerodynamic generalized forces in the form

$$\{\boldsymbol{Q}_A\} = \rho_\infty U_\infty [A_{\text{damp}}]\{\boldsymbol{q}_{,t}\} + \rho_\infty U_\infty^2 [A_{\text{stiff}}]\{\boldsymbol{q}\} \tag{51}$$

Equations (47) and (48) reveal that the matrix $[Q_{\text{stiff}}]$ is skew-symmetric and the matrix $[Q_{\text{damp}}]$ is symmetric.[36] Moreover, if the panel is made of a single material and has a constant thickness, then the aerodynamic damping matrix is proportional to the mass matrix.

Aeroelastic Stability Analysis

Using the expressions for generalized aerodynamic forces, the equations of motion for the panel are

$$[M]\{\ddot{\boldsymbol{q}}\} - \rho_\infty U_\infty [A_{\text{damp}}]\{\boldsymbol{q}\} + [K + K_G - \rho_\infty U_\infty^2 A_{\text{stiff}}]\{\boldsymbol{q}\} = \{\mathbf{0}\} \tag{52}$$

or

$$[\bar{\bar{M}}]\{\ddot{\boldsymbol{q}}\} + [\bar{\bar{C}}]\{\boldsymbol{q}\} + [\bar{\bar{K}}]\{\boldsymbol{q}\} = \{\mathbf{0}\} \tag{53}$$

Only aerodynamic damping is taken into account in the previous equations. If viscous structural damping is to be added, the matrix $[\bar{\bar{C}}]$ should be modified accordingly.[38,39]

At a given altitude, Mach number, and corresponding speed, and for a given set of in-plane loads obtained from a wing box stress solution for the maneuvering airplane (Ref. 32), the poles of the linear panel model can be found to determine whether the panel is aeroelastically stable or unstable. Laplace transforming Eq. (53) leads to

$$[[\bar{\bar{M}}]s^2 + [\bar{\bar{C}}]s + [\bar{\bar{K}}]]\{\boldsymbol{q}(s)\} = \{\mathbf{0}\} \tag{54}$$

This quadratic $N \times N$ eigenvalue problem can be solved either directly or by an equivalent first-order-generalized $2N \times 2N$ eigenproblem

$$s \begin{bmatrix} [I] & [0] \\ [0] & [\bar{\bar{M}}] \end{bmatrix} \begin{Bmatrix} \boldsymbol{x}_1 \\ \boldsymbol{x}_2 \end{Bmatrix} = \begin{bmatrix} [0] & [I] \\ -[\bar{\bar{K}}] & -[\bar{\bar{C}}] \end{bmatrix} \begin{Bmatrix} \boldsymbol{x}_1 \\ \boldsymbol{x}_2 \end{Bmatrix} \tag{55}$$

where

$$\{\boldsymbol{x}_1\} = \{\boldsymbol{q}\} \text{ and } \{\boldsymbol{x}_2\} = s\{\boldsymbol{q}\} \tag{56}$$

The problem can be written in simpler notation as

$$[\bar{U}]\{\boldsymbol{\phi}\} = \lambda[\bar{V}]\{\boldsymbol{\phi}\} \tag{57}$$

where λ, $\{\boldsymbol{\phi}\}$ is an eigenvalue/right-eigenvector pair, and the matrices $[\bar{U}]$, $[\bar{V}]$ are $2N \times 2N$ and are defined by Eqs. (52), (53), and (55).

Stability analysis at constant Mach number is carried out by gradually increasing the dynamic pressure and following the resulting movement of aeroelastic poles in the Laplace domain. A flutter instability (at the flutter dynamic pressure q_{flutter}) corresponds to a pole crossing the imaginary axis from the left to the right side of the s plane at some nonzero frequency. A divergence (buckling) instability corresponds to a pole crossing into the right-hand side of the s plane on the real axis (with zero frequency). When no damping is included in the mathematical model (either structural or aerodynamic), aeroelastic poles move on the imaginary axis as dynamic pressure is increased until a point q_{critical}, at which two poles coalesce and move off the imaginary axis to lie left and right of the imaginary axis.[1,2,36]

Analytic Sensitivities

Analytic sensitivities of stiffness and geometric stiffness matrices were presented in Ref. 32. Sensitivities with respect to thickness design variables and composite fiber angles have been obtained as well as sensitivities with respect to planform shape design variables. The key to obtaining analytic sensitivity expressions in our case is the explicit closed-form nature of the expressions for stiffness and geometric stiffness matrix terms. Analytic formulas are available for the area integrals [Eq. (24) and Ref. 30], and it is shown in Ref. 30 that the shape derivatives of members of the table of integrals $I_{\text{TR}}(m, n)$ can be expressed in terms of other members of the same table of integrals. Thus, once the table of integrals $I_{\text{TR}}(m, n)$ is generated (with m and n covering all powers required for aeroelastic analysis of the panel) it can be used for both analysis and sensitivity analysis.

Mass Matrix Sensitivities with Respect to Thickness Design Variables

The mass matrix is dependent on T_k^i, the sizing variable corresponding to the kth term of the ith layer, through the vector $\bar{\boldsymbol{T}}_k$ [Eqs. (27) and (28)]. The derivative of a mass matrix term is given as

$$\frac{\partial M_{\text{rs}}}{\partial T_k^i} = \frac{\partial M_{\text{rs}}}{\partial \bar{T}_k} \frac{\partial \bar{T}_k}{\partial T_k^i} \tag{58}$$

and based on the definition of $\bar{\boldsymbol{T}}_k$[Eq. (27)], then, for a given layer i and thickness term k

$$\frac{\partial \bar{\boldsymbol{T}}_k}{\partial T_k^i} = 1 \tag{59}$$

Substituting this back into Eq. (58) shows that differentiation with respect to the kth thickness term of any layer i is the same as differentiating the mass matrix with respect to the kth term of the overall thickness series

$$\frac{\partial M_{\text{rs}}}{\partial T_k^i} = \frac{\partial M_{\text{rs}}}{\partial \bar{T}_k} \tag{60}$$

Differentiating Eq. (30) for any specific k and i gives

$$\frac{\partial M_{\text{rs}}}{\partial T_k^i} = \frac{\partial M_{\text{rs}}}{\partial \bar{T}_k} = \rho_m \sum_{i=1}^{3} \sum_{j=1}^{6} \sum_{ii=1}^{3} \sum_{jj=1}^{6} U_i V_j U_{ii} V_{jj} \int\int_{\text{area}} x^m y^n \, dx \, dy \tag{61}$$

where

$$m = m_j^v + m_{jj}^v + m_r^w + m_s^w + m_k^t$$

$$n = n_i^u + n_{ii}^u + n_j^v + n_{jj}^v + n_r^w + n_s^w + n_k^t$$

Note that because of the linearity of the mass matrix in thickness design variables, if all $(\partial M_{\text{rs}}/\partial \bar{\boldsymbol{T}}_k)$ are calculated in advance, then the mass matrix can be formed as

$$M_{\text{rs}} = \sum_{k=1}^{N_t} \bar{\boldsymbol{T}}_k \frac{\partial M_{\text{rs}}}{\partial \bar{\boldsymbol{T}}_k} \tag{62}$$

This allows for the mass matrix and its thickness sensitivities to be calculated at the same time.

Mass Matrix Sensitivities with Respect to Shape Design Variables y_{LE}, y_{RE}, x_{FLI}, x_{FRI}, x_{ALI}, and x_{ARI}

The mass matrix is dependent on the shape variables through the coefficients U_i and V_j [Eqs. (5)] and the area integrals $I_{\text{TR}(m,n)}$. Analytical sensitivities for U_i and V_j are obtained through direct differentiation of Eqs. (5) and are listed in the Appendix. The derivatives of the area integrals I_{TR} with respect to x, where x is any shape variable, are prepared using Refs. 30 and 32. With this information, the derivative of the mass term M_{rs} is calculated as follows:

$$M_{\text{rs}} = \rho_m \sum_{k=1}^{N_t} \overline{\boldsymbol{T}}_k \sum_{i=1}^{3} \sum_{j=1}^{6} \sum_{ii=1}^{3} \sum_{jj=1}^{6} \left\langle U_i V_j U_{ii} V_{jj} \frac{\partial I_{\text{TR}(m,n)}}{\partial x} + \frac{\partial (U_i V_j U_{ii} V_{jj})}{\partial x} I_{\text{TR}(m,n)} \right\rangle \tag{63}$$

where

$$m = m_j^v + m_{jj}^v + m_r^w + m_s^w + m_k^t$$

$$n = n_i^u + n_{ii}^u + n_j^v + n_{jj}^v + n_r^w + n_s^w + n_k^t$$

Aerodynamic Matrix Shape Sensitivities

Shape derivatives of the aerodynamic damping and stiffness matrices are obtained by explicitly differentiating Eqs. (47) and (48):

$$\frac{\partial Q_{\text{stiff rs}}}{\partial x} = \cos\phi \sum_{i=1}^{3}\sum_{j=1}^{6}\sum_{ii=1}^{3}\sum_{jj=1}^{6} \cdot \left\{ \frac{\partial (U_i V_j U_{ii} V_{jj})}{\partial x} \times (m_{jj}^v + m_s^w) I_{\text{TR}(m-1,n)} + U_i V_j U_{ii} V_{jj} (m_{jj}^v + m_s^w) \frac{\partial I_{\text{TR}(m-1,n)}}{\partial x} \right\} + \sin\phi \sum_{i=1}^{3}\sum_{j=1}^{6}\sum_{ii=1}^{3}\sum_{jj=1}^{6} \left\{ \frac{\partial (U_i V_j U_{ii} V_{jj})}{\partial x} \times (n_{ii}^u + n_{jj}^v + n_s^w) I_{\text{TR}(m,n-1)} + U_i V_j U_{ii} V_{jj} (n_{ii}^u + n_{jj}^v + n_s^w) \frac{\partial I_{\text{TR}(m,n-1)}}{\partial x} \right\} \tag{64}$$

$$\frac{\partial Q_{\text{damp rs}}}{\partial x} = \sum_{i=1}^{3}\sum_{j=1}^{6}\sum_{ii=1}^{3}\sum_{jj=1}^{6} \left\{ \frac{\partial (U_i V_j U_{ii} V_{jj})}{\partial x} I_{\text{TR}(m,n)} + U_i V_j U_{ii} V_{jj} \frac{\partial I_{\text{TR}(m,n)}}{\partial x} \right\} \tag{65}$$

where the powers m, n are given by Eq. (49).

Recall from Eqs. (50) that the coefficients relating $[A_{\text{stiff}}]$ and $[A_{\text{damp}}]$ to $[Q_{\text{stiff}}]$ and $[Q_{\text{damp}}]$ are functions of the Mach number only. Therefore, the sensitivities of $[A_{\text{damp}}]$ and $[A_{\text{stiff}}]$ are

$$\frac{\partial A_{\text{stiff}}}{\partial DV} = \frac{1}{\sqrt{M_\infty^2 - 1}} \frac{\partial Q_{\text{stiff}}}{\partial DV} \tag{66}$$

$$\frac{\partial A_{\text{damp}}}{\partial DV} = \frac{1}{\sqrt{M_\infty^2 - 1}} \frac{M_\infty^2 - 2}{M_\infty^2 - 1} \frac{\partial Q_{\text{damp}}}{\partial DV} \tag{67}$$

Since $[Q_{\text{stiff}}]$ and $[Q_{\text{damp}}]$ are not affected by the Mach number, it is straightforward to obtain sensitivities with respect to Mach number, as follows:

$$\frac{\partial A_{\text{stiff}}}{\partial M_\infty} = \frac{\partial \left\langle \dfrac{1}{\sqrt{M_\infty^2 - 1}} \right\rangle}{\partial M_\infty} Q_{\text{stiff}} \tag{68}$$

$$\frac{\partial A_{\text{damp}}}{\partial M_\infty} = \frac{\partial \left\langle \dfrac{1}{\sqrt{M_\infty^2 - 1}} \dfrac{M_\infty^2 - 2}{M_\infty^2 - 1} \right\rangle}{\partial M_\infty} Q_{\text{damp}} \tag{69}$$

Eigenvalue Sensitivities

The eigenvectors $\{\boldsymbol{\phi}\}$ are defined in Eq. (57), and $\{\boldsymbol{\psi}\}$ are obtained from the adjoint eigenvalue problem

$$\{\boldsymbol{\psi}\}^T [\bar{\bar{U}}] = \lambda \{\boldsymbol{\psi}\}^T [\bar{\bar{V}}] \tag{70}$$

Differentiating Eq. (57) with respect to any design variable and premultiplying by the left eigenvectors, leads, after some rearrangement[24,32] to the derivative of an eigenvalue with respect to any design variable:

$$\frac{\partial \lambda}{\partial DV} = \frac{\{\boldsymbol{\psi}\}^T \left[\dfrac{\partial [\bar{\bar{U}}]}{\partial DV} - \lambda \dfrac{\partial [\bar{\bar{V}}]}{\partial DV} \right] \{\boldsymbol{\phi}\}}{\{\boldsymbol{\psi}\}^T [\bar{\bar{V}}] \{\boldsymbol{\phi}\}} \tag{71}$$

where the derivatives of the system matrices [Eqs. (52) and (55)] are obtained from

$$\frac{\partial [\bar{\bar{U}}]}{\partial DV} = \begin{bmatrix} [0] & [0] \\ -\dfrac{\partial [\bar{\bar{K}}]}{\partial DV} & -\dfrac{\partial [\bar{\bar{C}}]}{\partial DV} \end{bmatrix} \tag{72}$$

$$\frac{\partial [\bar{\bar{V}}]}{\partial DV} = \begin{bmatrix} [0] & [0] \\ [0] & \dfrac{\partial [\bar{\bar{M}}]}{\partial DV} \end{bmatrix} \tag{73}$$

where

$$\frac{\partial [\bar{\bar{M}}]}{\partial DV} = \frac{\partial [M]}{\partial DV} \tag{74}$$

$$\frac{\partial [\bar{\bar{C}}]}{\partial DV} = -\rho_\infty U_\infty \frac{\partial [A_{\text{damp}}]}{\partial DV} \tag{75}$$

$$\frac{\partial [\bar{\bar{K}}]}{\partial DV} = \frac{\partial [K]}{\partial DV} + \frac{\partial [K_G]}{\partial DV} - \rho_\infty U_\infty^2 \frac{\partial [A_{\text{stiff}}]}{\partial DV} \tag{76}$$

When aeroelastic stability constraints are imposed on the aeroelastic poles directly (in terms of the required amount of damping at given flight conditions[40]), the eigenvalue sensitivities determine the sensitivities of those constraints. However, as has already been discussed, in the case of linear panel flutter analysis, a mode coalescence criterion is often used for stability evaluation, in which case (ignoring structural and aerodynamic damping) poles reside on the imaginary axis in the s plane until instability occurs. In panel flutter optimization studies it has been more common to use a critical (or flutter) dynamic pressure constraint in search of an optimal panel with a given critical dynamic pressure.

Let the real and imaginary parts of the aeroelastic poles be given by

$$\lambda = \sigma + j\omega \tag{77}$$

The real part σ and the imaginary part ω are functions of dynamic pressure q_D, Mach number, and any sizing or shape design variables DV. At a given Mach number $\sigma = \sigma(q_D, DV)$ and at the critical (or flutter) dynamic pressure $\sigma = \sigma[q_{\text{flutter}}(DV), DV]$, defined at whatever value of damping used to determine flutter.

Differentiating with respect to DV and setting the derivative to zero to enforce the same flutter criterion

$$\frac{\partial \sigma}{\partial DV_{(\text{at-flutter})}} = \frac{\partial \sigma}{\partial DV} + \frac{\partial \sigma}{\partial q_{\text{flutter}}} \frac{\partial q_{\text{flutter}}}{\partial DV} = 0 \tag{78}$$

Thus

$$\frac{\partial q_{\text{flutter}}}{\partial DV} = -\frac{\left(\dfrac{\partial \sigma}{\partial DV} \right)}{\left(\dfrac{\partial \sigma}{\partial q_{\text{flutter}}} \right)} = -\frac{\text{Re}\left(\dfrac{\partial \lambda}{\partial DV} \right)}{\text{Re}\left(\dfrac{\partial \lambda}{\partial q_{\text{flutter}}} \right)} \tag{79}$$

The numerator is already known from Eq. (71). To obtain the denominator, Eq. (57) is differentiated with respect to dynamic pressure at the flutter dynamic pressure

$$\frac{\partial \lambda}{\partial q_{D(\text{at}:q=q_{\text{flutter}})}} = \frac{\{\boldsymbol{\psi}\}^T \left[\dfrac{\partial [\bar{\bar{U}}]}{\partial q_D} - \lambda \dfrac{\partial [\bar{\bar{V}}]}{\partial q_D} \right] \{\boldsymbol{\phi}\}}{\{\boldsymbol{\psi}\}^T [\bar{\bar{V}}] \{\boldsymbol{\phi}\}} \tag{80}$$

Or, for example, in the case of a given Mach number, where true airspeed becomes an explicit function of atmospheric density $U_\infty = U_\infty(\rho_\infty)$

$$\frac{\partial\lambda}{\partial\rho_\infty} = \frac{\{\psi\}^T\left[\frac{\partial[\bar{\bar{U}}]}{\partial\rho_\infty} - \lambda\frac{\partial[\bar{\bar{V}}]}{\partial\rho_\infty}\right]\{\phi\}}{\{\psi\}^T[\bar{\bar{V}}]\{\phi\}} \tag{81}$$

where

$$\frac{\partial[\bar{\bar{U}}]}{\partial\rho_\infty} = \begin{bmatrix} [0] & [0] \\ \dfrac{\partial(\rho_\infty U_\infty^2)}{\partial\rho_\infty}[A_{\text{stiff}}] & \dfrac{\partial(\rho_\infty U_\infty)}{\partial\rho_\infty}[A_{\text{damp}}] \end{bmatrix} \tag{82}$$

$$\frac{\partial[\bar{\bar{V}}]}{\partial DV} = \begin{bmatrix} [0] & [0] \\ [0] & [0] \end{bmatrix} \tag{83}$$

Some special cases may be encountered in the pole sensitivity analysis when multiple roots with nondistinct eigenvectors appear. The sensitivity of solutions in these cases is discussed in Refs. 41 and 42, and the sensitivities of the system matrices [Eqs. (72–76) and (82–83)], as given in the present work, still apply.

Test Cases and Results

Analysis Results

Before proceeding to study analytic sensitivities and approximations using the present capability, it is important to assess the accuracy of its panel flutter analysis results. For this, results of the present analysis technique for simply supported panels have been compared to reported results using other solution techniques for cases including skewed and trapezoidal shapes, yawed flow, isotropic and composite materials, variable composite fiber orientations, and a different combination of in-plane loads.[5,21,23] Convergence studies showed that while fourth-order polynomials in the Ritz series of Eq. (6) (not including the weight function F_B) were adequate in most cases, there were a few cases in which fifth-order polynomials were necessary. All following results, then, were based on a fifth-order polynomial multiplying the weight function in the displacement Ritz series.

Overall, the present polynomial-based technique was found to yield reliable results. A compilation of comparisons for a rich variety of cases can be found in Ref. 36. Correlations with the results of Ref. 23 are shown in this paper to demonstrate the capability of the present technique to calculate flutter dynamic pressures accurately for skewed, composite simply supported panels.

The simply supported panels studied in Ref. 23 are skewed, with skew angles (leading-edge sweep) varying from 0 to 45 deg. A unidirectional fiber composite material is used with fiber angle measured from the x axis (Fig. 2) and varying from 0 to 90 deg. Sides a and b of the panels are equal in length and the thickness is h. Material properties are $E1 = 137 \times 10^9$ Pa, $E2 = 9.7 \times 10^9$ Pa, $G12 = 5.5 \times 10^9$ Pa, $\nu_{12} = 0.3$, and $\rho_m = 1580$ kg/m^3.

Critical dynamic pressure and frequency are nondimensionalized as

$$\Lambda_{\text{crit}} = \frac{2q_{D\text{crit}}a^3}{E_2h^3\sqrt{M_\infty^2 - 1}}$$

$$\Omega_{\text{crit}} = \omega_{\text{crit}}a^2\sqrt{\frac{\rho_m}{E_2h^2}}$$

Both critical and flutter dynamic pressures have been calculated (no in-plane loads), and the comparison of critical dynamic pressure and critical frequency with the results of Ref. 23 are shown in Figs. 3 and 4.

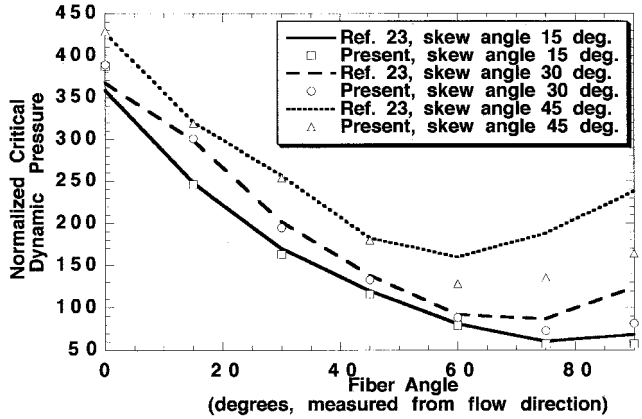

Fig. 3 Normalized critical dynamic pressure comparisons with Ref. 23 for a range of skew angles and fiber orientation angles.

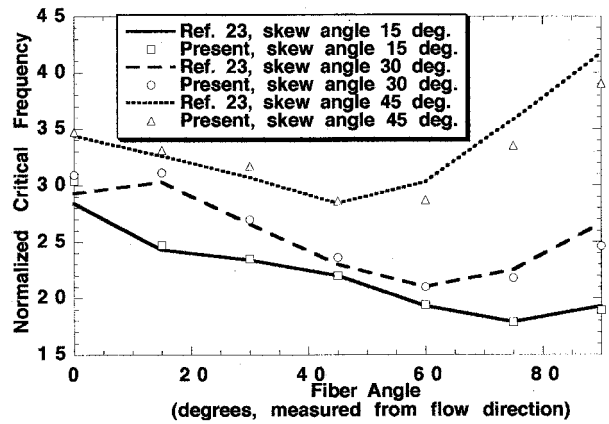

Fig. 4 Normalized critical frequency comparisons with Ref. 23 for a range of skew angles and fiber orientation angles.

As the figures show, the correlation is good over a considerable range of skew and fiber angles, except for cases in which skew angles and fiber angles are simultaneously large.

The good accuracy of the polynomial Ritz approach for buckling analysis of trapezoidal panels under combined in-plane loads has been demonstrated in Ref. 32. In the flutter analysis case discussed here, mass and aerodynamic matrices play an important role in addition to the stiffness and geometric stiffness matrices. To assess the accuracy of the polynomial Ritz flutter analysis in cases involving in-plane loading, results obtained with the present capability are compared with finite element results from Ref. 21. Square all-aluminum simply supported panels are analyzed, subject to different in-plane loadings. A nondimensional in-plane force is defined as

$$r_{ij} = (N_{ij}/\pi^2)(a^2/D)$$

and Table 1 summarizes the results, where the normalized critical dynamic pressure is defined by

$$\Lambda_{\text{crit}} = \frac{2q_{D\text{crit}}a^3}{D\sqrt{M_\infty^2 - 1}}$$

The correlation is good for moderate in-plane loading. In the case of N_{xy} loading (pure shearing), the correlation becomes worse as the intensity of in-plane loads increases.

Analytic Sensitivities and Approximations

With analytic derivatives available, as shown by the previously discussed derivations, it is possible to assess the accu-

Table 1 Normalized critical dynamic pressures[a] for aluminum square panels under in-plane loads

r_{ij}[b]	Ref. 21	Present	% difference
$r_{xx} = -3$	275.7	265.1	3.85
$r_{xx} = 0$	518.2	512.6	1.08
$r_{xx} = 3$	789.0	793.1	0.5
$r_{xy} = 2$	487.0	473.1	2.85
$r_{xy} = 4$	418.9	381.7	8.9
$r_{xy} = 6$	321.5	274.3	14.7

[a] $\Lambda_{crit} = 2q_{Dcrit}a^3/D\sqrt{M_\infty^2 - 1}$.
[b] $r_{ij} = (N_{ij}/\pi^2)(a^2/D)$.

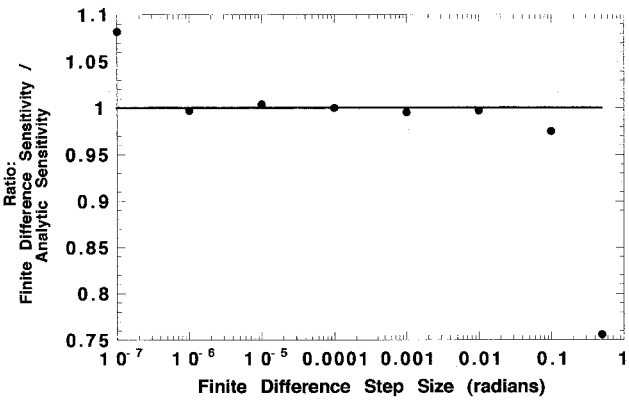

Fig. 5 Effect of step size on the accuracy of finite difference derivatives. Base design: a skewed composite square panel with a skew angle of 15 deg and fiber angle of 45 deg.

racy of finite difference derivatives and examine the range of acceptable step sizes. As has been shown for the case of polynomial Ritz analysis of wing box structures,[30] ill conditioning (when high-order polynomials are used) can lead to erroneous finite difference derivatives, even in cases when the analysis itself is adequate. In all panel flutter analysis cases studied here, and with the order of Ritz polynomials used, no ill-conditioning problems were encountered. Figure 5 shows the accuracy of first-order finite difference derivatives as a function of the step size used for the case of varying material fiber direction on a composite skewed panel (the case with a skew angle of 15 deg and fiber angle of 45 deg in Fig. 3). The behavior function considered is the critical dynamic pressure. As can be seen, a large range of finite difference steps yield accurate finite difference derivatives.

Finite difference derivatives were used to verify the analytic derivatives for a variety of cases including different design variables (thickness, material, and shape) and different behavior functions (such as aeroelastic poles or, alternatively critical and flutter dynamic pressures). Using the analytic derivatives, it became possible to examine first-order Taylor-series approximations in various cases and to gain some experience as to the move limits that might be required.

In Fig. 6, for example, the calculated analytic sensitivity of flutter dynamic pressure with respect to fiber angle is used to construct direct and reciprocal first-order approximations[24] for a 15-deg skewed panel of Ref. 23.

In Fig. 7, a direct first-order Taylor approximation is constructed based on the analytic sensitivity of flutter dynamic pressure with respect to a magnification factor applied to the system of combined in-plane loads on a skewed panel. An isotropic panel with a skew angle of 30 deg, equal sides of 1 m, and thickness of 3 mm is subject to $N_x = -2000$ and $N_y = -1000$ N/m. The geometric stiffness matrix corresponding to this in-plane loading is $[K_G]_{REF}$, and the in-plane loads are varied so that the actual geometric stiffness matrix is $[K_G]$ = eta $\times$ $[K_G]_{REF}$ (eta is a multiplication factor increasing or decreasing a system of in-plane loads). It is easy to obtain the derivative of $[K_G]$ with respect to eta in this case, and the results simulate a situation where aeroelastic stability of a skin panel is influenced by changes in load distribution in the larger structure containing this panel.

As a final example a skin panel is studied (Fig. 8), subject to a change in planform geometry that affects both in-plane loads and panel characteristics. This will be the case when skin panels on a wing or fuselage change shape because of changes in spar/rib locations or the overall shape of the airplane.

The panel starts with a skew angle of 30 deg and is made of a single-fiber composite layer with fiber orientation of 15 deg with respect to the x axis (thickness is 3 mm). An in-plane load of N_{xx} starts as 0.5 of the buckling load (at X_{AR} =

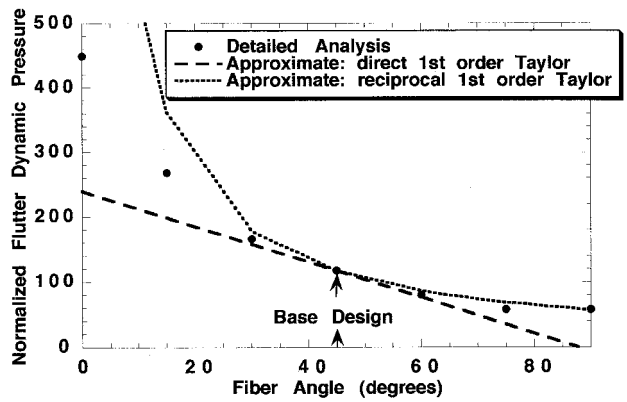

Fig. 6 Detailed analysis and first-order Taylor-series approximations of normalized flutter dynamic pressure for a skewed composite panel. Skew angle: 15 deg.

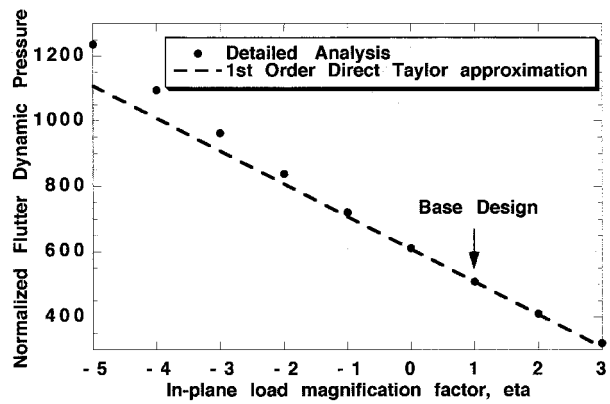

Fig. 7 Linear direct Taylor-series approximation of panel flutter dynamic pressure for a 30-deg skewed panel, subject to a varying system of in-plane loads. Eta is a multiplication factor increasing or decreasing a system of in-plane loads based on $N_x = -2000$, $N_y = -1000$ N/m.

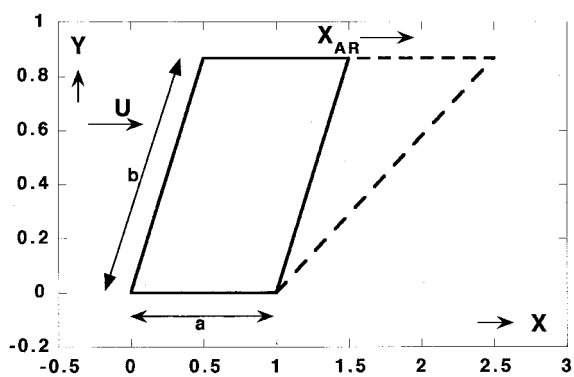

Fig. 8 Planform shape variation of aluminum wing box panel subject to in-plane loading (dimensions are in meters).

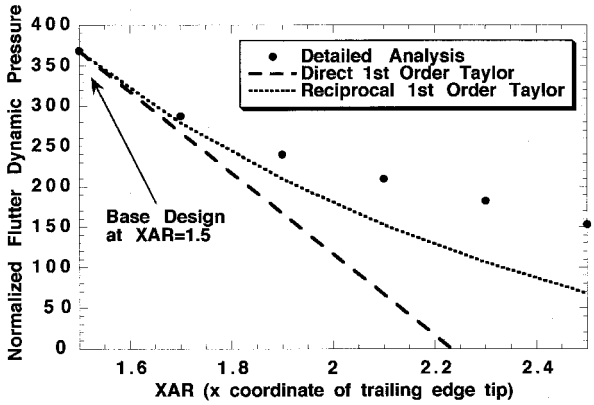

Fig. 9 Detailed analysis and first-order Taylor-series approximations of normalized flutter dynamic pressure for a variable shape aluminum panel (XAR varying) on an aluminum wing box. In-plane loads, N_{xx}, vary with XAR.

1.5 m) and changes linearly to 0.65 of the buckling load when X_{AR} reaches 2.5 m.

Derivatives of the flutter dynamic pressure are obtained using the derivative with respect to X_{AR} when N_{xx} is fixed, and then augmenting with the derivative caused by changes in N_{xx} (affecting the geometric stiffness). Direct and reciprocal Taylor-series approximations are shown in Fig. 9.

Conclusions

The capability to include configuration shape-design variables, in any multidisciplinary design optimization of airplanes in the conceptual or preliminary design stages, is essential. Developments in recent years advanced the state of the art in DOSA, covering approximate stress, deformation, structural dynamic and buckling analysis as well as analytical behavior sensitivity techniques, where wing box structures and skin panel structures, are subject to shape as well as material and sizing variations. The present work has focused on the design-oriented aeroelastic analysis of optimized skin panels in supersonic flow. Since, in typical optimum aeroelastic synthesis of wing structures, many skin panels can be buckling-critical, and since stressing a panel up to a point close to its buckling load may have a considerable effect on its aeroelastic stability, it becomes important to develop efficient analysis and sensitivity capabilities for panel flutter constraints.

It is shown in this work how modeling and Ritz formulations based on simple polynomial functions in global coordinates lead to the efficient evaluation of panel stiffness, geometric stiffness, and mass, as well as aerodynamic damping and aerodynamic stiffness matrices. Using analytic formulas for area integrals of polynomial terms over general trapezoidal area shapes, it is shown that no numerical integration is needed for evaluating panel structural or aerodynamic matrices. A table of area integrals for the panel, including area integrals over the panel of terms of the form $x^m * y^n$, needs to be evaluated only once for a given panel shape (in Refs. 30 and 32). Then, structural and aerodynamic matrices, as well as their analytic sensitivities with respect to sizing, material, and shape design variables, can be obtained by linear combinations of members of this table of integrals.

Systematic evaluation of the resulting panel flutter prediction capability was carried out, comparing results from the present work with results from other references. Overall, the current capability led to good correlation with other prediction techniques up to panel leading-edge sweep angles of 30 deg. Differences in panel flutter boundary predictions between the current technique and other analysis techniques, including finite elements, were observed for panel sweep angles of more than 30 deg. Additional work is needed in this area to find out whether the discrepancies are caused by limitations of the current polynomial Ritz analysis or the other analysis techniques used for comparison. Unfortunately, only a few articles on panel flutter address the aeroelastic stability of panels of general trapezoidal shapes.

Expressions for analytic sensitivity of panel aeroelastic poles and resulting flutter dynamic pressure have been obtained and checked against finite difference sensitivities. Excellent correlations and a wide range of step sizes adequate for the finite difference derivatives have been found. Used, in turn, in direct and reciprocal Taylor-series approximations for the flutter dynamic pressure, the flutter and sensitivity results have been shown to lead to quite robust approximations over a wide range of design variable changes (wide move limits). The work has also shown how to integrate the panel aeroelastic analysis and sensitivity predictions with a wing box analysis and sensitivity capability, where in-plane loads determined by the wing box behavior serve as inputs to the panel aeroelastic behavior. Shape variations of the wing and its internal structure affect the panel both via its in-plane loads and directly through the effects of its shape on its structural and aerodynamic matrices.

Appendix: Shape Derivatives of U_i and V_j Terms

Derivatives with respect to X_{FR}:

$$\frac{\partial U_1}{\partial x_{FR}} = \frac{\partial U_2}{\partial x_{FR}} = \frac{\partial U_3}{\partial x_{FR}} = \frac{\partial V_4}{\partial x_{FR}} = 0$$

$$\frac{\partial V_1}{\partial x_{FR}} = \frac{-y_L}{y_R - y_L} R_A$$

$$\frac{\partial V_2}{\partial x_{FR}} = \frac{y_L}{y_R - y_L}$$

$$\frac{\partial V_3}{\partial x_{FR}} = \frac{-y_L}{y_R - y_L} \cdot S_A + R_A \cdot \frac{1}{y_R - y_L} \tag{A1}$$

$$\frac{\partial V_5}{\partial x_{FR}} = -\frac{1}{y_R - y_L}$$

$$\frac{\partial V_6}{\partial x_{FR}} = \frac{1}{y_R - y_L} \cdot S_A$$

Derivatives with respect to Y_L, y_R, x_{FL}, x_R, x_{AL}, and x_{AR} (Fig. 2) are obtained by explicit direct differentiation of Eqs. (1), (2), and (5), and yield similar closed-form expressions.

Acknowledgments

The work reported here was supported by the National Science Foundation through a National Young Investigator Award and by NASA Ames Research Center. This support is gratefully acknowledged.

References

[1]Dowell, E. H., *Aeroelasticity of Plates and Shells*, Noordhoff International, Leyden, The Netherlands, 1975.

[2]Librescu, L., *Elastostatics and Kinetics of Anisotropic and Heterogenous Shell Type Structures*, Noordhoff International, Leyden, The Netherlands, 1975.

[3]Dugundji, J., "Theoretical Consideration of Panel Flutter at High Supersonic Mach Numbers," *AIAA Journal*, Vol. 4, No. 7, 1966, pp. 1257–1266.

[4]Eastep, F. E., and McIntosh, S. C., "Analysis of Nonlinear Panel Flutter and Response Under Random Excitation or Nonlinear Aerodynamic Loading," *AIAA Journal*, Vol. 9, No. 3, 1971, pp. 411–418.

[5]Sander, G., Bon, C., and Geradin, M., "Finite Element Analysis of Supersonic Panel Flutter," *International Journal for Numerical Methods in Engineering*, Vol. 7, 1973, pp. 379–394.

[6]Yang, T. Y., "Flutter of Flat Finite Element Panels in Supersonic Unsteady Potential Flow," *AIAA Journal*, Vol. 13, No. 11, 1975, pp. 1502–1507.

[7]Bismarck-Nasr, M. N., "Finite Element Analysis of Aeroelasticity

of Plates and Shells," *Applied Mechanics Reviews*, Vol. 45, No. 12, 1992, pp. 461–482.

[8]Ibrahim, R. A., Orono, P. O., and Madaboosi, S. R., "Stochastic Flutter of a Panel Subjected to Random In Plane Forces, Part I: Two Mode Interaction," *AIAA Journal*, Vol. 28, No. 4, 1990, pp. 694–702.

[9]Liaw, D. G., "Supersonic Flutter of Laminated Thin Plates with Thermal Effects," *Journal of Aircraft*, Vol. 30, No. 1, 1993, pp. 105–111.

[10]Shore, C. P., "Flutter Design Charts for Biaxially Loaded Isotropic Panels," *Journal of Aircraft*, Vol. 7, No. 4, 1970, pp. 325–329.

[11]Lin, K.-J., Lu, P.-J., and Tarn, J.-Q., "Flutter Analysis of Composite Panels Using High Precision Finite Elements," *Computers and Structures*, Vol. 33, No. 2, 1989, pp. 561–574.

[12]Chowdary, T. V. R., Parthan, S., and Sinha, P. K., "Finite Element Flutter Analysis of Laminated Composite Panels," *Computers and Structures*, Vol. 53, No. 2, 1994, pp. 245–251.

[13]Shiau, L.-C., and Chang, J.-T., "Transverse Shear Effect on Flutter of Composite Panels," *Journal of Aerospace Engineering*, Vol. 5, No. 4, 1992, pp. 465–479.

[14]Lee, I., and Cho, M.-H., "Supersonic Flutter Analysis of Clamped Composite Panels Using Shear Deformable Finite Elements," *AIAA Journal*, Vol. 29, No. 5, 1991, pp. 782, 783.

[15]Hajela, P., and Glowasky, R., "Application of Piezoelectric Elements in Supersonic Panel Flutter Suppression," AIAA Paper 91-3191, Sept. 1991.

[16]Scott, R. C., and Weishaar, T. A., "Controlling Panel Flutter Using Adaptive Materials," AIAA Paper 91-1007, April 1991.

[17]Dowell, E. H., and Ilgamov, M., *Studies in Nonlinear Aeroelasticity*, Springer–Verlag, New York, 1988.

[18]Sipcic, S. R., and Morino, L., "Dynamic Behavior of Fluttering Two-Dimensional Panels on an Airplane in Pull-Up Maneuver," *AIAA Journal*, Vol. 29, No. 8, 1991, pp. 1304–1312.

[19]Frampton, K. D., Clark, R. L., and Dowell, E. H., "State Space Modeling for Aeroelastic Panels Subject to Linearized Potential Flow Aerodynamic Loading," *Proceedings of the AIAA/ASME/ASCE/AHS/ASC 36th Structures, Structural Dynamics, and Materials Conference* (New Orleans, LA), Vol. 2, AIAA, Washington, DC, 1995, pp. 1183–1189.

[20]Durvasula, S., "Flutter of Simply Supported, Parallelogrammic, Flat Panels in Supersonic Flow," *AIAA Journal*, Vol. 5, No. 9, 1967, pp. 1668–1673.

[21]Kariappa, Somashekar, B. R., and Shah, C. G., "Discrete Element Approach to Flutter of Skew Panels with In-Plane Forces Under Yawed Supersonic Flow," *AIAA Journal*, Vol. 8, No. 11, 1970, pp. 2017–2022.

[22]Srinivasan, R. S., and Babu, J. C., "Free Vibration and Flutter of Laminated Quadrilateral Plates," *Computers and Structures*, Vol. 27, No. 2, 1987, pp. 297–304.

[23]Chowdary, T. V. R., Sinha, P. K., and Parthan, S., "Finite Element Flutter Analysis of Composite Skew Panels," *Computers and Structures*, Vol. 58, No. 3, 1996, pp. 613–620.

[24]Haftka, R. T., and Gurdal, Z., *Elements of Structural Optimization*, 3rd ed., Kluwer, Dordrecht, The Netherlands, 1992, Chaps. 6 and 7.

[25]Craig, R. R., "Optimization of a Supersonic Panel Subjected to a Flutter Constraint—A Finite Element Solution," *AIAA Journal*, Vol. 16, No. 3, 1979, pp. 404, 405.

[26]Weisshaar, T. A., "Aeroelastic Optimization of a Panel in High Mach Number Supersonic Flow," *Journal of Aircraft*, Vol. 9, No. 9, 1972, pp. 611–617.

[27]Weisshaar, T. A., "Panel Flutter Optimization—A Refined Finite Element Approach," *International Journal for Numerical Methods in Engineering*, Vol. 10, No. 1, 1976, pp. 77–91.

[28]Van Keuren, G. M., and Eastep, F., "Use of Galerkin's Method for Minimum Weight Panels with Dynamic Constraints," *Journal of Spacecraft and Rockets*, Vol. 14, No. 7, 1977, pp. 414–418.

[29]Librescu, L., and Beiner, L., "Weight Minimization of Orthotropic Flat Panels Subjected to a Flutter Speed Constraint," *AIAA Journal*, Vol. 24, No. 6, 1986, pp. 991–997.

[30]Livne, E., "Analytical Sensitivities for Shape Optimization in Equivalent Plate Structural Wing Models," *Journal of Aircraft*, Vol. 31, No. 4, 1994, pp. 961–969.

[31]Harvey, M. S., "Automated Finite Element Modeling of Wing Structures for Shape Optimization," M.S. Thesis, Dept. of Aeronautics and Astronautics, Univ. of Washington, Seattle, WA, Nov. 1993.

[32]Livne, E., and Milosavljevic, R., "Analytic Sensitivity and Approximation of Skin Buckling Constraints in Wing Shape Synthesis," *Journal of Aircraft*, Vol. 32, No. 5, 1995, pp. 1102–1113.

[33]Singhvi, S., and Kapania, R. K., "Analytical Shape Sensitivities and Approximations of Modal Response of Generally Laminated Tapered Skew Plates," *Proceedings of the AIAA/ASME/ASCE/AHS/ASC 33rd Structures, Structural Dynamics and Materials Conference*, April 1992, pp. 1858–1869.

[34]Livne, E., and Li, W.-L., "Aeroservoelastic Aspects of Wing/Control Surface Planform Shape Optimization," *AIAA Journal*, Vol. 33, No. 2, 1995, pp. 302–311.

[35]Li, W.-L., and Livne, E., "Analytic Sensitivities and Approximations in Supersonic and Subsonic Wing/Control Surface Unsteady Aerodynamics," AIAA Paper 95-1219, April 1995.

[36]Mineau, D., "Flutter Analysis and Analytic Sensitivities for Trapezoidal Panels," M.S. Thesis, Dept. of Aeronautics and Astronautics, Univ. of Washington, Seattle, WA, March 1996.

[37]Giles, G. L., "Equivalent Plate Modeling for Conceptual Design of Aircraft Wing Structures," AIAA Paper 95-3945, Sept. 1995.

[38]Voss, H. M., and Dowell, E. H., "Effect of Aerodynamic Damping on Flutter of Thin Plates," *AIAA Journal*, Vol. 2, No. 1, 1964, pp. 119, 120.

[39]Lottati, I., "The Role of Damping on Supersonic Panel Flutter," *AIAA Journal*, Vol. 23, No. 10, 1985, pp. 1640–1642.

[40]Hajela, P., "A Root Locus Based Flutter Synthesis Procedure," *Journal of Aircraft*, Vol. 20, No. 12, 1983, pp. 1021–1027.

[41]Pedersen, P., and Seyranian, A., "Sensitivity Analysis for Problems of Dynamic Stability," *International Journal of Solids and Structures*, Vol. 19, No. 4, 1983, pp. 315–335.

[42]Seyranian, A., "Sensitivity Analysis of Multiple Eigenvalues," *Mechanical Structures and Machines*, Vol. 21, No. 2, 1993, pp. 261–284.